Heliyon 10 (2024) e29222

Contents lists available at ScienceDirect

Heliyon

journal homepage: www.cell.com/heliyon

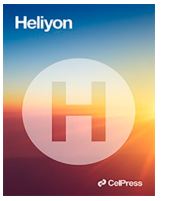

Research article

Modeling of gas sensor based on zinc oxide thin films by feedback loop using operational amplifier

Raju Bhattarai [a,*], Rishi Ram Ghimire [a], Deependra Das Mulmi [b], Ram Bahadur Thapa [a]

[a] Patan Multiple Campus, Department of Physics, Patandhoka, Lalitpur, Nepal
[b] Nepal Academy of Science and Technology, Khumaltar, Lalitpur, Nepal

ARTICLE INFO

Keywords:
Miniatured sensing device
Less energy consuming
Noble electronic model

ABSTRACT

Nanostructured Zincoxide thin-film is widely used as a sensing material because of its tunable surface microstructure and wide optical bandgap but synthesizing a film with desired value of resistance and reproducibility of film is challenging, particularly by chemical method. In this work, we showed how a ZnO film of arbitrary resistance can be used as a sensor without application of heat using operational amplifier. Zinc oxide thin film was synthesized by using the Sol-gel method (Spin coating) and was characterized by XRD and SEM which revealed wurtzite polycrystalline nature of Zinc oxide film with average grain size 17–25 nm. In this report, we designed a noble electronic circuit capable of detecting analyte gas molecule even if very small change in film resistance occurs due to the influence of gas molecule. In recently available sensors, the quality of the film degrades over time due to repeated heating and cooling, resulting in a reduced lifetime for the sensor. To address this issue and achieve higher sensitivity, as well as to fabricate an affordable, portable, precise, energy-efficient and durable device, this electronic model offers advantages over classical temperature-dependent sensors.

1. Introduction

Currently, gas sensing is seeking the attention of both industries and academia because of its wide-ranging application in the areas like industrial production (e.g., detection of methane in mines), automotive industry (e.g., detection of pollutant gases from vehicles), medical applications (e.g., electronic noses simulating the human olfactory system), supervision of indoor air quality (e.g., carbon monoxide detection), environmental studies (e.g., monitoring greenhouse gas). Since the last sixty years, researches have been focused on investigation of different types of sensing materials, sensing mechanism and, fabrication techniques of sensing materials. Those researches revealed various fabrication techniques, introduced several sensing materials (e.g., different metal-oxides, polymers) and different approaches of sensing mechanism [1].

Mostly, the gases are sensed by the particular materials due to variation in electrical, optical, acoustic, chromatographic and calorimetric properties of sensing materials in influence of various gases. In case of metal oxide semiconductor thin films, nanotubes and polymers, the electrical property, i.e. resistance of the film, varies due influence of respective gases [2]. By monitoring this change in value of resistance of the film, a perfect gas sensor can be built.

* Corresponding author.
E-mail address: bhattarairaaju@gmail.com (R. Bhattarai).

https://doi.org/10.1016/j.heliyon.2024.e29222
Received 19 September 2023; Received in revised form 1 April 2024; Accepted 3 April 2024
Available online 10 April 2024

Various nanostructured materials such as thin film, nanowire, nanotube, and nanopowder, composed of different materials including metals, semiconductors, and polymers, are widely utilized in fabricating gas sensors. Among these, metal oxide semiconductor is considered one of the strong candidates for sensors and detectors, with ZnO being particularly promising due to its wide abundance, eco-friendliness, cost-effectiveness, and tunable surface morphology [1]. However, despite being an excellent candidate for gas sensors, ZnO suffers from a serious drawback: slow response times, difficulty in maintaining desired resistance and challenges in sensing at room temperature.

To overcome these discrepancies, one needs to modify the synthesis process of the material to achieve a high-quality film with the desired resistance suitable for sensing purposes. In this work, we have designed a simple electronic circuit connected with a ZnO film of arbitrary resistance. This circuit assists in detecting even small fractional changes in the resistance of the film due to the influence of reducing gases using an operational amplifier. This technique has enabled us to avoid the need for advanced and expensive synthesis processes to achieve a desired resistance. This technique can apply to realize a sensor using a film grown by any method and any value of resistance.

Most metal oxide-based gas sensors require maintenance at a specific operating temperature to achieve higher sensitivity. For example, MQ sensors utilize an inbuilt heating system to raise the temperature of sensing material to a range of 200 °C–300 °C for effective sensing. These sensors cannot function independently; instead, they must be connected to an Arduino-UNO and cannot be powered by a small battery source alone. Additionally, they require a significant warm-up time to function optimally [3]. Extended use of the sensor film at high temperatures may alter its surface microstructure over time, leading to inconsistencies in sensor performance and potential damage to the film and device. Therefore, operating the sensor at room temperature is preferable to mitigate these issues. Our electronic circuit addresses this challenge by eliminating temperature dependency, resulting in a cost-effective, portable, precise, energy-efficient, and durable sensing device. This approach represents an emerging and highly sought-after technique in gas sensing applications today.

2. Methodology

Gas sensing properties of various metal oxide semiconductors were studied through published journals and variation in resistance of different materials were noted. Different electronic circuits were designed using CircuitMod 2.7 and Online Circuit Simulator and Schematic Editor-Circuit Lab. Then the variation in output of the designed circuit due to change in resistance of the variable resistor (Thin Film) was tabulated and analyzed. For the experimental verification, single coated Zinc Oxide thin films were fabricated using spin coating method.

2.1. Fabrication of thin film

There are more than a dozen of methods: Laser ablation, Physical vapor decomposition, Melt mixing, Sputter deposition, Electric arc deposition, Ion implantation, Precipitation method, Co-precipitation method, Colloidal methods, Sol-gel processing (Spin coating, Dip coating and Spray pyrolysis), Water-oil micro-emulsion method, Hydrothermal synthesis, Solvothermal, Sono-chemical synthesis, Polyol methods, Vapor phase fabrication, etc for thin film fabrication [4,5]. Because of its simplicity, reliability and accessibility, we found Spin Coating method being feasible within our budget and lab frame too.

Spin Coating is the most preferred technique for the thin film deposition onto flat substrate due to its plainness, low cost, easy doping, low operating temperature and spin and film thickness controllability. A very small amount of coating material is dropped at the centre of the substrate spinning at a constant speed or at rest, and then is rotated at high speed to spread the material uniformly all over the substrate. As soon as, the coating is completed, the substrate is annealed for the evaporation of the unwanted solvent and deposition of the film. The process is continued until the desired thickness or resistance of the film is achieved [6,7].

Glass substrates were cut into square pieces (2.5 cm × 2.5 cm), washed with distilled water then sonicated for 15 min with distilled water and Acetone at 70°C then dried in a hot air oven at 100°C. For 0.5 M precursor solution (Solution for pure ZnO thin film), 13.3872 g of Zinc Acetate Dihydrate (ZAD) and 6 mL of Diethyl Amine (DEA) added to 120 mL of Ethanol was stirred at 300 rpm for an hour at room temperature. 0.1 mL of precursor solution was spread over the spinning (at 3000 rpm for 30 s) substrate in a spin coater

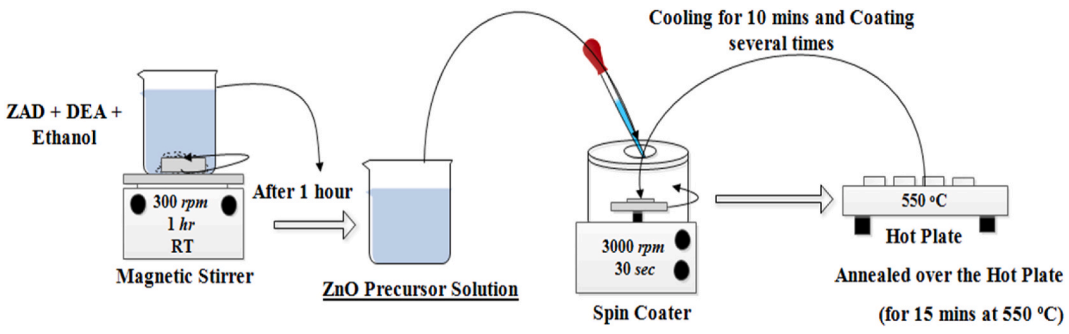

Fig. 1. Preparation of ZnO thin film by Spin Coating Method.

and was annealed over the hot plate at 550°C for 15 min as illustrated in Fig. 1.

The films fabricated were further cut into minute pieces (4 mm × 7 mm) and heated at 100°C for 2 h. Upon heating, thin insulated wires-conducting at the ends were connected to both the ends of the film using Silver paste. Two heating systems were adjusted at the ends of a cylinder of the volume of about 300 cm^3; heater at the top was to monitor the temperature of the film (if necessary) and heater at the bottom was to evaporate liquid (if necessary). This is the way, how we built a setup for the exposure of thin film to gas for sensing purpose. The needle of the syringe was adjusted as shown as in Fig. 2 so as to pass gas or drop liquid over the heater.

Different concentrations of ethanol and methanol were passed into the chamber and corresponding response of the circuit was observed and noted.

2.2. Circuit (sensor) designing

Several electronic circuits were designed using CircuitMod 2.7 and Online Circuit Simulator and Schematic Editor called Circuit Lab. The variation of outputs resulting from changes in resistance of thin film used in the circuit was analyzed. Then the necessary electronic components were soldered onto the PCB board.

Two resistors labelled R_1 and R_2) as shown in Fig. 3 were connected in series with a 3 V battery. The positive input terminal of first amplifier was linked to the junction of R_1 and R_2 and the negative input terminal was joined to the connecting point of feedback resistor (R_f) and film resistor (R_x). The output terminal of the first amplifier was connected back to its negative input terminal through a feedback resistor and also to non-inverting input terminal of second amplifier as illustrated as in Fig. 3. For second amplifier, its inverting input terminal was connected to positive terminal of the battery, positive input terminal was connected to output terminal of first amplifier. Two light emitting diodes (LED), one red and the other green were connected in anti-parallel configuration (anode of red joined to cathode of green and vice-versa) between the outputs of first and second amplifiers with cathode of red LED connected to output of first amplifier. The seventh pins of both amplifiers were connected to positive terminal of source; fourth pins were grounded, while the first and eighth pins were left floating. Additionally, a burger was connected in series with red LED.

Also, the configuration works if the both amplifiers and LEDs are flipped with respect to polarity.

2.3. Sensing mechanism

The detection mechanism of Semiconductor Metal Oxide (SMO) as a sensor is complex and not yet fully understood. Adsorption ability, electrophysical and chemical properties, catalytic activity, thermodynamic stability and the adsorption/desorption properties of the surface of SMO as well yields this complexity [1]. ZnO (n-type semiconductor) thin film surface, when exposed to air, adsorb oxygen molecules to form molecular type adsorbate (O_2, O_2^-) and dissociative type (O_2^{2-}) adsorbate ions forfeiting electrons from the conduction band, yielding electron-depleted space-charge layer in the grain boundary region which leads to large surface potential barrier and large resistance. The target gas (ethanol/methanol) may undergo dehydration and dehydrogenation and successively oxidized to CO, CO_2 and H_2O, but ZnO being basic oxide, dehydrogenation is favored. The response of the film towards alcohol vapors is dependent on the conversion of alcohol into aldehydes [7,8].

$$2C_2H_5OH \rightarrow 2CH_3CHO + H_2 \quad (1)$$

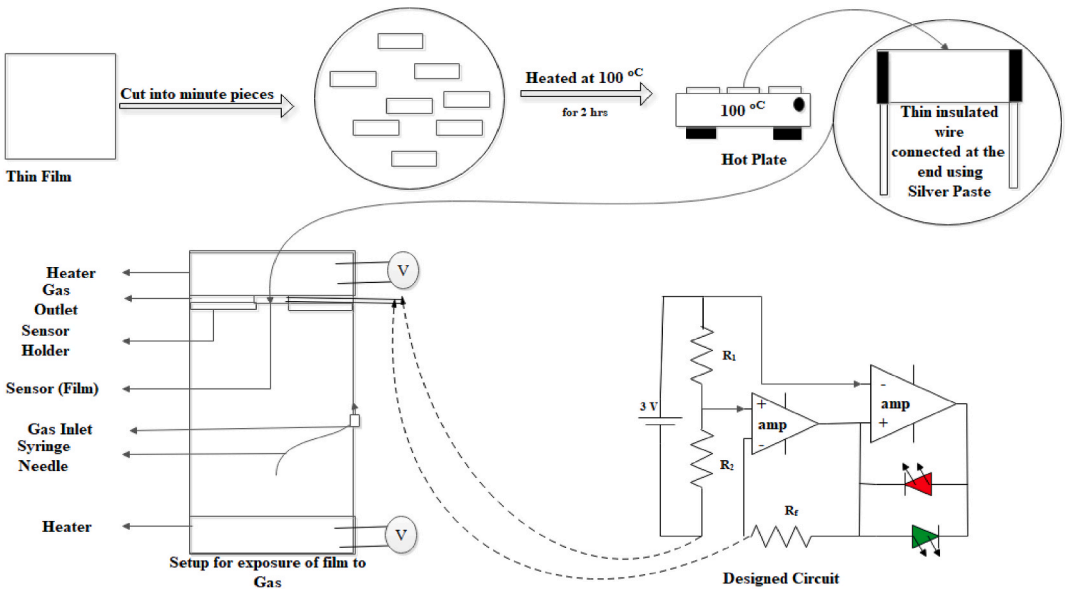

Fig. 2. Entire setup for sensing.

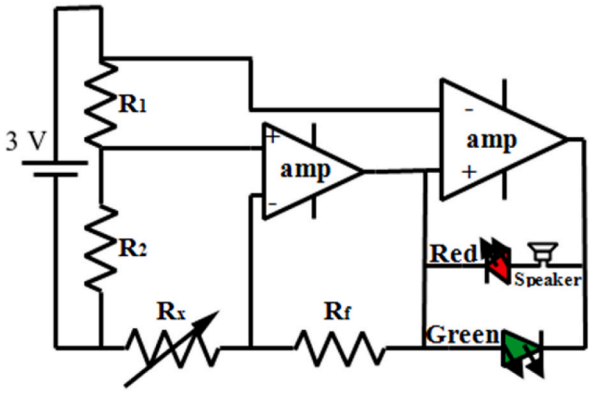

Fig. 3. Designed Sensor Circuit where R_x is film resistance.

$$2CH_3CHO\ (ad) + 5O_2^{2-}\ (ad) \rightarrow 4CO_2 + 4H_2O + 10e^- \quad (2)$$

$$2C_2H_5OH\ (ad) + O_2^{2-}\ (ad) \rightarrow 2C_2H_4O^-\ (ad) + 2H_2O \quad (3)$$

$$C_2H_4O^-\ (ad) \rightarrow CH_3CHO\ (ad) + e^- \quad (4)$$

$$CH_3OH\ (g) \rightarrow CH_3OH\ (ad) \rightarrow CH_3O\ (ad) + H(ad) \quad (5)$$

The release of electrons back to the film enhances the conductivity of the film and deduces the resistance [8]. The oxygen adsorbed onto the film surface traps electrons from the bulk of material forming a potential barrier. When the adsorbed oxygen is replaced by reducing gas molecules the barrier at the grain boundaries decreases consequently reduces the electrical resistance of the film [1]. This reduces potential at the negative input terminal of the first amplifier which yields change in its output and potential at the positive input terminal of the second amplifier. This change in the value of positive input of the second amplifier changes the polarity of its output from negative to positive and current flows through red LED only. So, only red LED glows and burger beeps.

In the former case, when the film is not exposed to reducing gas, the circuit yields negative output. This causes the red LED to be reverse biased, blocking electron to flow through it while the green LED, being forward biased, allows current flow through it and glows. Once the vapor dissipates, the film promptly resumes its adsorption of atmospheric oxygen, returning to its original state [8]. Consequently, the circuit once again emits a green glow once the film has recovered.

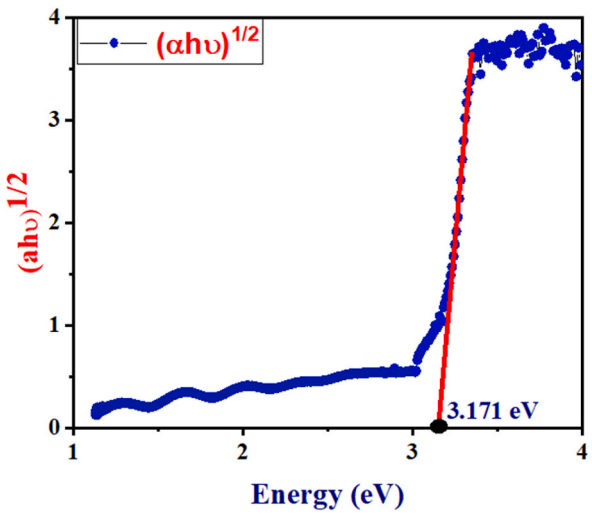

Fig. 4. Tauc's Plot for calculation of Energy Bandgap.

3. Results and discussion

3.1. UV–Vis spectroscopy

The optical characterization of the samples was performed in Nepal Academy of Science and Technology (NAST) using UV–Vis spectrophotometer (Carry 60 spectrophotometer, Agilent Technology). The absorbance and transmittance of the films were measured which were further analyzed in Fig. 4 to calculate the band gap and thickness of the films. For indirect transition, the variation in absorption coefficient with the photon energy obey Tauc's plot method,

$$(\alpha h\nu)^{0.5} = A\left(h\nu - E_g\right) \tag{6}$$

where A is a constant, E_g is the optical band gap, h is the plank constant and α is the absorption coefficient. Extrapolation of $(\alpha h\nu)^{0.5} = 0$ yields the optical bandgap energy of the films [9].

The bandgap of thin film fabricated by us was found to be 3.171 eV.

3.2. X-ray diffraction (XRD)

The dual natured (behaving as both particle and wave) electromagnetic radiation having high penetration power [6], photon energy within 100 eV- 100 KeV is termed as X-ray. It is a non-destructive technique used for characterizing crystalline substance. This helps in the identification and quantification of the crystalline phase, structure, orientation, composition and defects. Further, it is used to measure the size, strain or micro-strain effects, transparency and electron mobility in thin-films [10]. The structural characterizations of fabricated thin films were analyzed using XRD [Bruker D2 Phaser X-ray diffractometer of CuKα radiation (wavelength: 1.54184 Å)] at 40 KV of operating voltage and current of 40 mA in the 2θ range of 20^o - 80^o at scanning rate of 15^o per minute at NAST, Khumaltar, Lalitpur, Nepal as shown in Fig. 5. The Debye Scherrer's formula used to calculate the average grain size 'D' is given by,

$$D = \frac{0.9\lambda}{\beta \cos\theta} \tag{7}$$

where, 0.9 is the correction factor, λ is the wavelength of the x-radiation, β is the full width at half maximum (FWHM) of the observed peak and θ is the Bragg's angle [10]. Comparing calculated d-spacings with the standard JCPDS values of card number 36–1451, the observed peaks were indexed. The average crystallite size of ZnO was found to be 20.068 nm using Scherrer's method.

The crystallite size of deposited ZnO thin films were also calculated using W–H plot method using prominent XRD planes then compared with that obtained from Scherrer's formula. The W–H plot is related with the full width half maxima (FWHMs) (β) of XRD peaks and crystallite size (D) through the relation,

$$\frac{\beta \cos\theta}{\lambda} = \frac{1}{D} + \frac{4\varepsilon \sin\theta}{\lambda} \tag{8}$$

where, ε is the amount of residual strain, θ is the angle of diffraction, λ is the wavelength of X-ray [10]. A graph between βcosθ/λ versus 4sinθ/λ when plotted and fitted linearly as shown in Fig. 6, the reciprocal of the x-intercept gives the average crystallite size [11] and was found to be 17.345 nm.

The crystallite size of the fabricated film calculated from the W–H plot was found consistent with that as calculated from Scherrer's

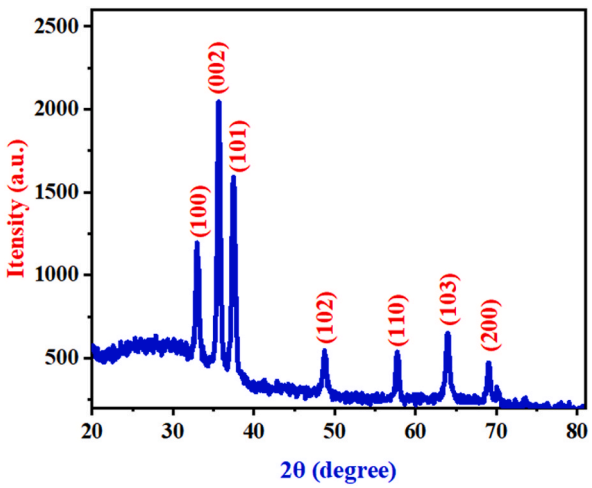

Fig. 5. XRD pattern of Pristine ZnO thin film.

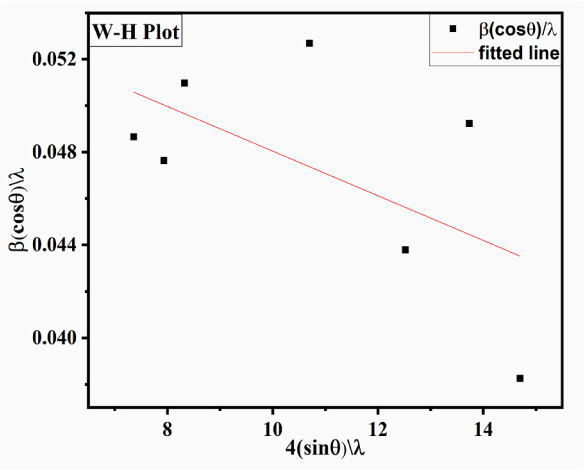

Fig. 6. William-Hall (W–H) plots of pristine ZnO.

method as tabulated in Table 1.

3.3. Scanning Electron Microscope (SEM) and EDX analysis

The surface morphology of ZnO thin films were performed using Scanning Electron Microscope at Research Centre for Eco-Environment Sciences, Chinese Academy of Sciences, Beijing, China.

Fig. 7a and (b), shows the SEM images of undoped ZnO with scale 1 μm and 500 nm and magnification of 50K and 100K respectively. The SEM image depicts grainy structure of film. The average grain size of ZnO was found to be around 25 nm which is quite corresponding to results obtained from XRD analysis.

Fig. 8 shows the EDX spectra which assure that the film is of Zinc oxide. Very small peak of Aluminium is detected which may be due to Aluminium silicate (glass) substrate. The EDX spectrum of ZnO sample as figured in Table 2 shows the high content i.e. 65.37 wt % of Zinc, 32.29 wt % of Oxygen and 4.34 wt % of Aluminium which is almost negligible compared to oxygen and Zinc.

3.4. Circuital analysis

The circuit designed is the novel concept in sensing gas. Since the resistance of the film is influenced by material used for depositing thin film, the number of coating done, doping in film and aging of the film, the values of the resistors used in the circuit must be different for different value of film resistance at the ordinary condition. These values of the components must be appropriate to determine or sense the selected reducing gas. Here we present some particular values of these components and the critical point value of the film resistance (value of film resistance beyond which the output voltage of the circuit changes its polarity or the LEDs switch) for the particular configuration of the circuit. We analyzed the circuit fixing the feedback resistance and the ratio (R_1: R_2) and manually changing the value of film resistance unless we obtained critical value.

The film resistance of quite higher value than the critical value should be used for better sensing. Considering this, best range of the film was estimated and their corresponding sensitivity was calculated using the relation:

$$S = \frac{R_x - R_g}{R_x} \tag{9}$$

where, S is sensitivity, R_x is film resistance before exposure to gas and R_g is the value resistance of film after exposure to gas.

Table 1
Shows XRD analysis for miller indices, d-spacing and grain size of the deposited ZnO thin film.

S.N.	Miller Indices	Angle 2θ	Calculated d (Å)	JCPDS(36–1451) d (Å)	Crystallite Size D(nm)		
					Scherrer's Method		W–H plot
1.	(100)	32.95075	2.7172	2.8142	19.31788	Average	
2.	(002)	35.60633	2.5204	2.6033	19.73324	20.0678	17.3445
3.	(101)	37.42934	2.4018	2.4759	18.44347		
4.	(102)	48.69692	1.8692	1.9111	17.84351		
5.	(110)	57.69607	1.5972	1.6247	21.46739		
6.	(103)	63.92009	1.4559	1.4771	19.09518		
7.	(200)	69.00289	1.3605	1.4072	24.57326		

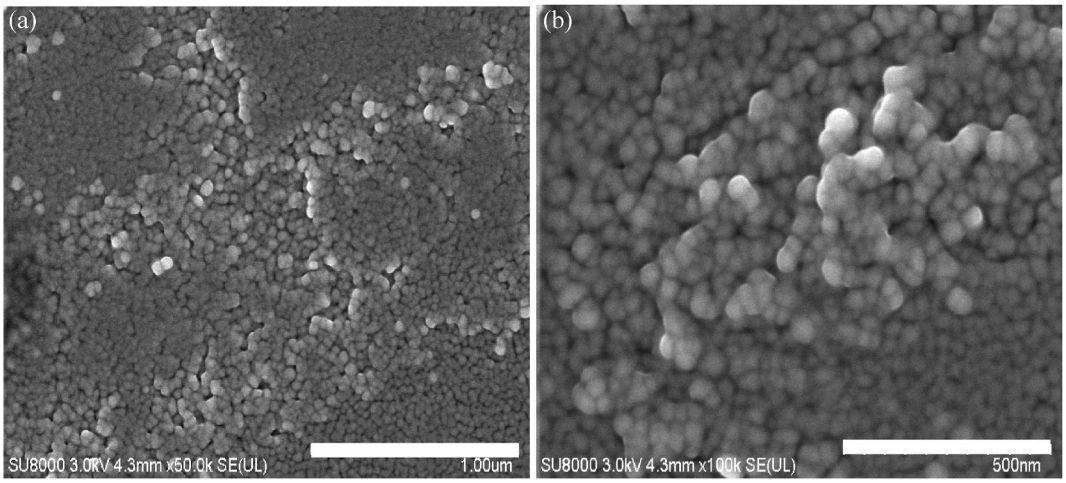

Fig. 7. SEM images of ZnO thin film with scale (a) 1 μm and (b) 500 nm.

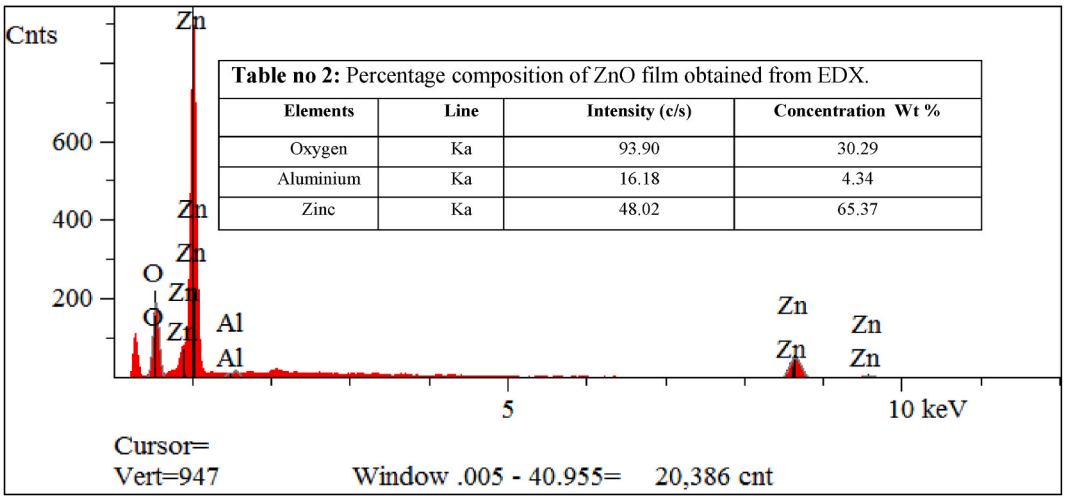

Table no 2: Percentage composition of ZnO film obtained from EDX.

Elements	Line	Intensity (c/s)	Concentration Wt %
Oxygen	Ka	93.90	30.29
Aluminium	Ka	16.18	4.34
Zinc	Ka	48.02	65.37

Fig. 8. Energy Dispersive X-ray image of Pristine ZnO film.

Table 2
Percentage composition of ZnO film obtained from EDX.

Elements	Line	Intensity (c/s)	Concentration Wt %
Oxygen	Ka	93.90	30.29
Aluminium	Ka	16.18	4.34
Zinc	Ka	48.02	65.37

Table no 3 represents the theoretical values for the circuital components for sensing the selected gas to approximate the appropriate value of feedback resistor, the ratio of R_1 and R_2 to be used in the circuit for sensing particular gas within a limited range of sensitivity. Further the tables, eases to choose the sensor components accordance to resistance of fabricated film. We need to select the sensitivity within which we are willing to work with. This helps finding the critical value using relation (4) and helps to approximate the feedback resistance and ratio R_1:R_2. Clearly, ratio of feedback resistance and critical value seems roughly equal to ratio R_1:R_2.

After fabrication of thin-film, we can measure film resistance and analyzing table no 3 and Fig. 9, we will be able.

In the sensitivity stacked chart, Fig. 9a, b and 9c, for different ratio R_1:R_2 and different feedback resistance above, film resistance from which sensitivity is measured, is mentioned at the top of it. If we use the film of above mentioned resistance as sensor, and corresponding values of feedback resistance and ratio R_1:R_2, the sensitivity of the film on exposure to gas must be as indicated on green block so as to sense it. In other words, the exposure to gas should reduce the film resistance by indicated values to detect the gas. These suggest that for higher film resistance, we should use higher value of feedback resistor or large R_1:R_2 for more sensitive sensor and for

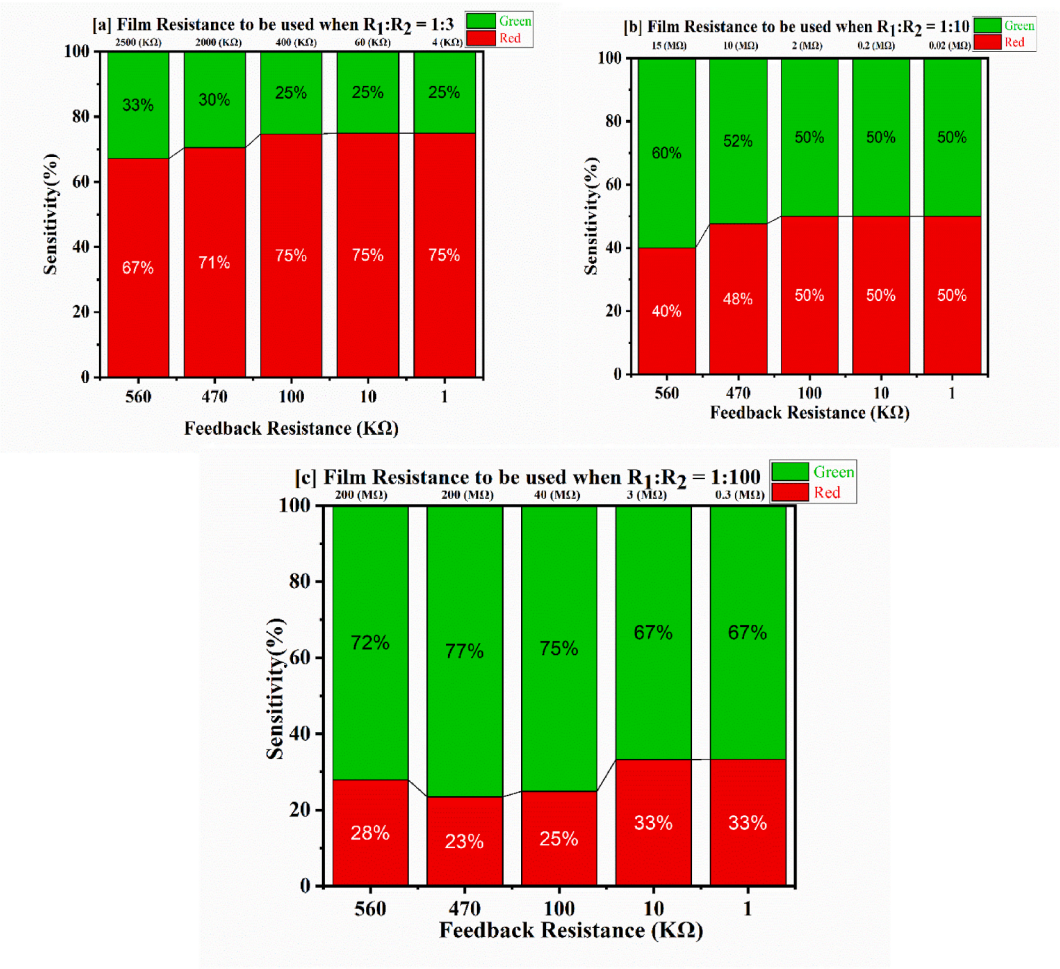

Fig. 9. Sensitivity Stacked Chart for different ratio of R_1 and R_2 (a) 1:3, (b) 1:10 and (c) 1:100 and different values of Film and Feedback Resistances.

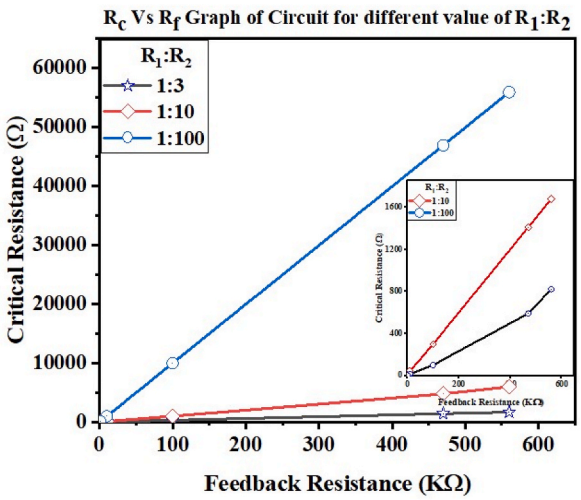

Fig. 10. Critical vs feedback resistance graph at different ratio of R_1 and R_2.

film resistance with low resistance, comparably small values of the components can be used.

Fig. 10 clearly depicts that critical point value or the critical resistance of the film is linearly dependent on the feedback resistance used in the circuit for same R_1:R_2. The critical resistance is such value of the film above which the circuit glows Green and below which results glowing Red. Also, it suggests that increment in the ratio R_1:R_2 yields higher value of critical resistance which will be very efficient for using highly resistive film as a sensor. Lower value of R_1:R_2 gives lower value of critical resistance which will be more effective if used with less resistive film. Furthermore, highly resistive film can be used as sensor along with lower value of R_1:R_2 if the target gas highly reduces the film below critical value. The mechanism is same for feedback resistor. Thus, appropriate value of R_1:R_2 and feedback resistor can let us sense reducing gas of any concentration.

Fig. 11 is the plot of film resistance (in log scale) vs least percentage change required for sensing the target gas at different value of feedback resistance for R_1:R_2 equals 1:100. The graph clearly shows that highly resistive film needs more than 90% change in their film resistance for sensing (RED glow in circuit) in above mentioned configuration. But Film resistance closer to the critical value of resistance can sense well within less percentage change in its former value. This circuit best suits for sensing even if the target gas increases the film resistance. But selecting appropriate and accurate R_1:R_2, feedback resistor and remaining circuital components is most for excellence performance.

Thus, analyzing Figs. 10 and 11, we can conclude that sensitivity of the circuit is dependent on the value of critical resistance of the film but not on the film resistance. This is the most fantabulous characteristics of the circuit which overcomes the dependency of the available ordinary sensors on film resistance. Furthermore, the critical value of the film is controllable. It depends upon the components used in the circuit. The film resistance may vary from few KΩ to hundreds of MΩ and no chemical synthesis yields film of desired resistance with accuracy which has brought complexion in sensing with desired accuracy. Thus, the noble circuit designed is the ultimate way to eradicate this drawback of the ordinary sensor. Finally, designation of sensor can be summed up as:

(i) Measuring film resistance after fabrication R_x).
(ii) Choosing sensitivity (S).
(iii) Calculating Critical Resistance using selected sensitivity and Film Resistance as:

$$R_c = R_x - \frac{S \times R_x}{100} \tag{10}$$

(iv) Choosing appropriate value of R_1:R_2, R_f and other circuital components and fabricating sensor.

3.5. Experimental verification

This was experimentally verified using alcohol (ethanol and methanol) vapors as reducing gas and ZnO as sensing material in the film. The value of the fabricated film resistance was more than 200 MΩ, ratio (R_1: R_2) was 1: 3, the value of feedback resistance was 560 KΩ and two eight pins chips (UA741CN) were used as amplifiers. Two LEDs (one red and another green) were fixed as shown in the circuit. 9 V battery was used as a source for two amplifier chips and another 3 V battery was conned in series with R_1 and R_2. The film was exposed to different concentrations of gas (alcohol vapors) and corresponding change was noted. The Table 4 represents the experimental values.

The Table 4 clearly shows the switching of potential at output of circuit due to exposure of alcohol vapors. This confirms that the designed circuit senses alcohol vapor (reducing gas) using pristine zinc oxide thin film.

3.6. Response and recovery

Response and recovery time are another indispensable factor for determining whether or not a sensor is reliable. Here we have tabulated response and recovery time of our circuital sensor after exposure to different concentration of ethanol and methanol vapors in Table 5.

The circuit remains in either normal state/zone (glowing Green) or in detection zone (glowing Red). When the target gas is passed, sooner the film resistance decreases and reaches the critical resistance, the circuit changes its state from normal and when the gas passes by, film resistance starts increasing again. As soon as it exceeds R_c, it changes its state back to normal. The time for which the circuit remains in either state while responding to different concentrations of Ethanol and Methanol vapors is shown below in Fig. 12:

The Fig. 12 clearly depicts that higher the concentration, longer it stays in detection zone. Further, for same concentration, circuit responds faster to ethanol than methanol.

The vapors were passed simultaneously into the sensor setup and were free to escape at any time. The variation in film resistance in response to 50, 250 and 500 ppm of Ethanol and Methanol vapors were observed and are graphed as shown in Fig. 13a and b. The graph reflects that the resistance of the film while responding reducing gases decreases rapidly for few seconds then slows down and reaches its minimum value. The minimum value is attained when the target gases replace maximum number of reduced oxygen molecules in the grain boundary of film. As soon as the impact of the gas diminishes, the oxygen molecules in reduced form starts gathering at the grain boundary region and the film resistance starts increasing again. Its obvious that lower the concentration, less is the impact on film resistance.

Clearly, the experimental result shows that the film is sustainable and is very sensitive to reducing gases. The longevity of recovery time as observed in Fig. 14 may be due to poor ventilation for gas outlet in our experimental setup.

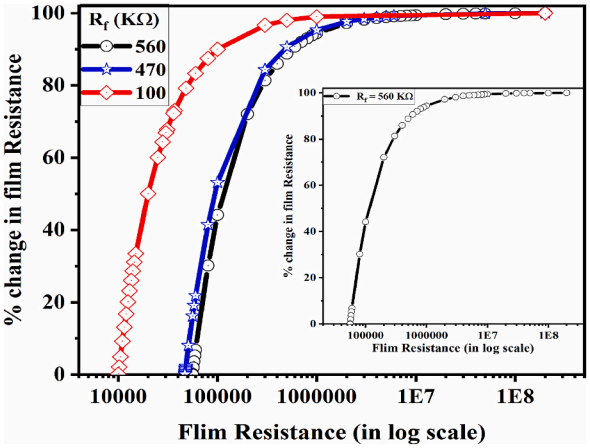

Fig. 11. Least percentage change of Film Resistance required for sensing vs Film resistance graph for different value of R_f.

Table 3
Shows the values of Components to be used in accordance to film resistances and selected gas.

S.N.	Feedback Resistance R_f (KΩ)	Ratio (R_1: R_2)	Critical Point Value (KΩ)	Best Range of Film Resistance R_x	Minimum Sensitivity S (%)
1.	560	1:3	1679	(2–1.7) MΩ	(15–1.24)
	560	1:10	5999	(10-6) MΩ	(40–0.02)
	560	1:100	55899	(200-56) MΩ	(72–0.18)
2.	470	1:3	1410	(2–1.5) MΩ	(30-5)
	470	1:10	4759	(15-5) MΩ	(67–4.82)
	470	1:100	46899	(200-47) MΩ	(77–0.22)
3.	100	1:3	298.99	(400-300) KΩ	(25–0.34)
	100	1:10	999.79	(2-1) MΩ	(50–0.021)
	100	1:100	9982.56	(40-10) MΩ	(75–0.174)
4.	10	1:3	44.98	(80-45) KΩ	(44–0.04)
	10	1:10	99.98	(300-100) KΩ	(67–0.02)
	10	1:100	997.92	(3-1) MΩ	(67–0.02)
5.	1	1:3	2.999	(5-3) KΩ	(40–0.03)
	1	1:10	9.998	(30-10) KΩ	(67–0.02)
	1	1:100	99.82	(300-100) KΩ	(67–0.18)

Table 4
Value of Input and Output Voltages of Circuit before and after exposure to alcohol vapors.

S.N.	Gas	Concentration (ppm)	Potential (V)			
			Before passing gas		After passing gas	
			Input	Output	Input	Output
1.	Ethanol	500	0.35	−4.15	6.27	2.56
		250	0.36	−4.15	5.11	2.28
		50	0.35	−4.14	4.12	2.13
2.	Methanol	500	0.36	−4.14	5.56	2.52
		250	0.34	−4.15	4.92	2.23
		50	0.36	−4.13	3.98	2.06

4. Conclusions

The innovative circuit proposed for gas sensing utilizes a zinc oxide thin film to detect reducing gases effectively. Once the thin film is fabricated, its resistance becomes known. By referring to Table 3, Figs. 10, and Fig. 11, we can determine the optimal values for the feedback resistor and the ratio of R_1 to R_2 to be employed in the circuit for sensing specific gases within a predefined sensitivity range.

Moreover, the electrical components utilized are readily available in compact sizes on the market. This enables us to create a portable, miniaturized sensing device or sensor at a low cost while consuming minimal energy, all thanks to the implementation of the zinc oxide thin film. Additionally, the circuit lends itself to straightforward breathalyzer testing applications.

Table 5
Response and Recovery time of ZnO thin-film varying with concentration and types of alcohol.

S.N.	Alcohol	Concentration (ppm)	Response Time (s)	Recovery Time (s)
1.	Ethanol	500	2	60
		250	4	28
		50	6	10
2.	Methanol	500	2	80
		250	5	35
		50	8	15

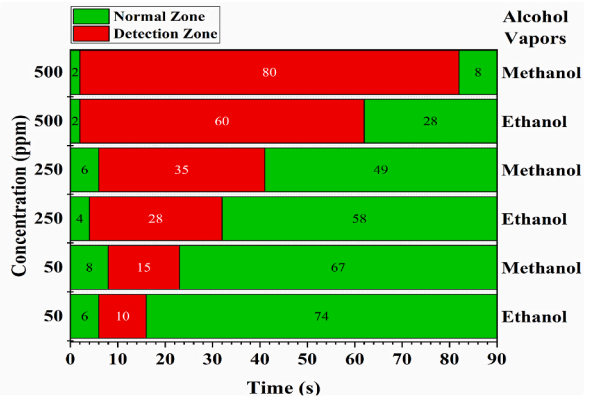

Fig. 12. Time for which the circuit remains in either state in response to different concentration of alcohol vapors.

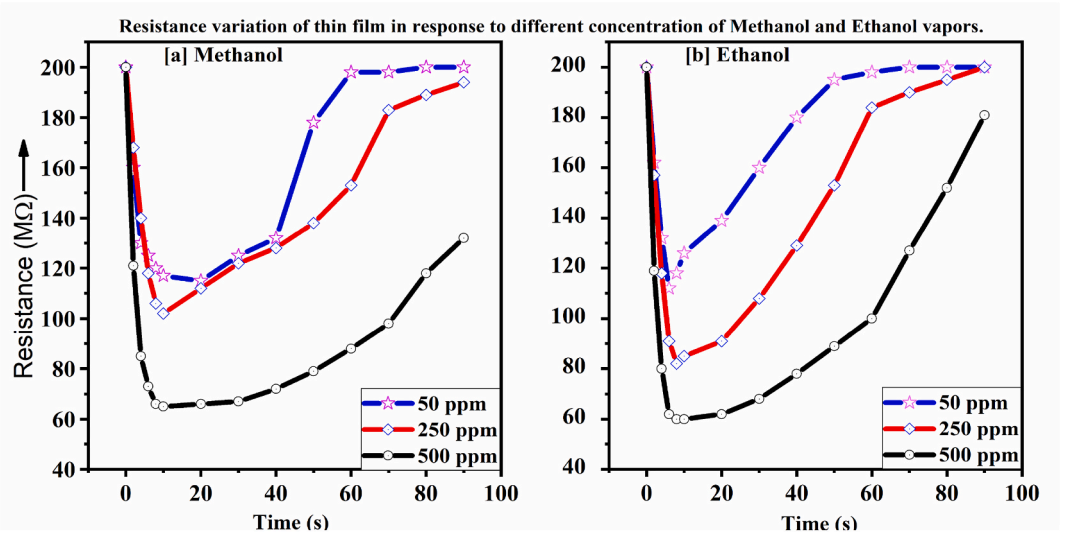

Fig. 13. Variation of film resistance in response to various concentrations of Alcohol vapors.

Data availability statement

The data that support the findings of this research are openly available in [Sensor-Data] at the link below: https://github.com/raaju1993/Sensor-Data.
Feel free to analyze it according to the specific data sharing practices and requirements of your study.

CRediT authorship contribution statement

Raju Bhattarai: Writing – review & editing, Writing – original draft, Visualization, Software, Resources, Project administration, Methodology, Investigation, Funding acquisition, Formal analysis, Data curation, Conceptualization. **Rishi Ram Ghimire:** Validation,

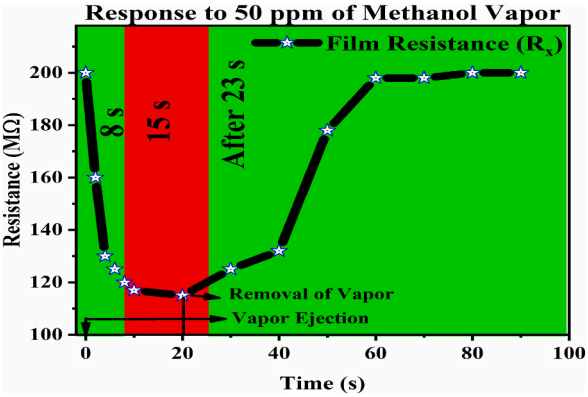

Fig. 14. Film response to 50 ppm of Methanol Vapors.

Supervision, Investigation. **Deependra Das Mulmi:** Validation, Supervision. **Ram Bahadur Thapa:** Methodology, Investigation, Formal analysis.

Declaration of competing interest

The authors declare that they have no known competing financial interests or personal relationships that could have appeared to influence the work reported in this paper.

Acknowledgments

We will always be grateful to Patan Multiple Campus (PMC) and Nepal Academy of Science and Technology (NAST) for providing us a platform to our research work. One of the authors; Raju Bhattarai would like to express sincere thanks to Trilochan Khanal and Tirtha Narayan Shah, Patan Multiple Campus for providing essential electronic components.

Appendix A. Supplementary data

Supplementary data to this article can be found online at https://doi.org/10.1016/j.heliyon.2024.e29222.

References

[1] X. Liu, S. Cheng, H. Liu, S. Hu, D. Zhang, H. Ning, A survey on gas sensing technology, Sensors 12 (7) (2012) 9635–9665.
[2] S. Kanan, O. El-Kadri, I. Abu-Yousef, M. Kanan, Semiconducting metal oxide-based sensors for selective gas pollutant detection, Sensors 9 (10) (2009) 8158–8196.
[3] Z. Yu, L. Fang, L. Deqin, G. Bingqian, Monitoring the spontaneous combustion of coal stack based on ZigBee and Lab view, J. Phys. Conf. 1303 (2019).
[4] A. Naveed Ul Haq, A. Nadhman, I. Ullah, G. Mustafa, M. Yasinzai, I. Khan, Synthesis approaches of zinc oxide nanoparticles: the dilemma of ecotoxicity, J. Nanomater. 2017 (2017).
[5] A. Mohammed, P.S. Naik, S.S. Suryavanshi, L.I. Nadaf, Design and fabrication of low cost and miniaturized setup for gas sensor, IOSR J. Appl. Phys. 7 (2) (2015) 2278–4861.
[6] H.E. Unalan, P. Hiralal, N. Rupesinghe, S. Dalal, W.I. Milne, G.A. Amaratunga, Rapid synthesis of aligned zinc oxide nanowires, Nanotechnology 19 (25) (2008) 255608.
[7] X. Jiaqiang, H. Jianjun, Z. Yuan, S. Yu'an, X. Bing, Studies on alcohol sensing mechanism of ZnO based gas sensors, Sensor. Actuator. B Chem. 132 (2008) 334–339.
[8] S.C. Navale, V.R.S. Mulla, S.W. Gosavi, S.K. Kulkarni, Sensor. Actuator. B Chem. 126 (2) (2007) 382–386.
[9] D.D. Mulmi, B. Dahal, H.-Y. Kim, M.L. Nakarmi, G. Panthi, Optical and photocatalytic properties of lysozyme mediated titanium dioxide nanoparticles, Optik 154 (2018) 769–776.
[10] F. F Garcés, N. Budini, R. Koropecki, R. Arce, Structural analysis of ZnO (: Al, Mg) thin films by X-ray diffraction, Procedia Materials Science 8 (2015) 551–560.
[11] S.H. Chaki, M.D. Chaudhary, M. Deshpande, SnS thin films deposited by chemical bath deposition, dip coating and SILAR techniques, J. Semiconduct. 37 (5) (2016) 053001.